Taylor & Francis
Taylor & Francis Group

Inhalation Toxicology

International Forum for Respiratory Research

ISSN: 0895-8378 (Print) 1091-7691 (Online) Journal homepage: http://www.tandfonline.com/loi/iiht20

Molecular mechanisms of pulmonary response progression in crystalline silica exposed rats

Rajendran Sellamuthu, Christina Umbright, Jenny R. Roberts, Shih-Houng Young, Diana Richardson, Walter McKinney, Bean T. Chen, Shengqiao Li, Michael Kashon & Pius Joseph

To cite this article: Rajendran Sellamuthu, Christina Umbright, Jenny R. Roberts, Shih-Houng Young, Diana Richardson, Walter McKinney, Bean T. Chen, Shengqiao Li, Michael Kashon & Pius Joseph (2017) Molecular mechanisms of pulmonary response progression in crystalline silica exposed rats, Inhalation Toxicology, 29:2, 53-64, DOI: 10.1080/08958378.2017.1282064

To link to this article: http://dx.doi.org/10.1080/08958378.2017.1282064

INHALATION TOXICOLOGY, 2017
VOL. 29, NO. 2, 53–64
http://dx.doi.org/10.1080/08958378.2017.1282064

Taylor & Francis
Taylor & Francis Group

RESEARCH ARTICLE

Molecular mechanisms of pulmonary response progression in crystalline silica exposed rats

Rajendran Sellamuthu, Christina Umbright, Jenny R. Roberts, Shih-Houng Young, Diana Richardson, Walter McKinney, Bean T. Chen, Shengqiao Li, Michael Kashon and Pius Joseph

Health Effects Laboratory Division, National Institute for Occupational Safety and Health (NIOSH), Morgantown, WV, USA

ABSTRACT

An understanding of the mechanisms underlying diseases is critical for their prevention. Excessive exposure to crystalline silica is a risk factor for silicosis, a potentially fatal pulmonary disease. Male Fischer 344 rats were exposed by inhalation to crystalline silica (15 mg/m^3, six hours/day, five days) and pulmonary response was determined at 44 weeks following termination of silica exposure. Additionally, global gene expression profiling in lungs and BAL cells and bioinformatic analysis of the gene expression data were done to understand the molecular mechanisms underlying the progression of pulmonary response to silica. A significant increase in lactate dehydrogenase activity and albumin content in BAL fluid (BALF) suggested silica-induced pulmonary toxicity in the rats. A significant increase in the number of alveolar macrophages and infiltrating neutrophils in the lungs and elevation in monocyte chemoattractant protein-1 (MCP-1) in BALF suggested the induction of pulmonary inflammation in the silica exposed rats. Histological changes in the lungs included granuloma formation, type II pneumocyte hyperplasia, thickening of alveolar septa and positive response to Masson's trichrome stain. Microarray analysis of global gene expression detected 94 and 225 significantly differentially expressed genes in the lungs and BAL cells, respectively. Bioinformatic analysis of the gene expression data identified significant enrichment of several disease and biological function categories and canonical pathways related to pulmonary toxicity, especially inflammation. Taken together, these data suggested the involvement of chronic inflammation as a mechanism underlying the progression of pulmonary response to exposure of rats to crystalline silica at 44 weeks following termination of exposure.

ARTICLE HISTORY
Received 10 November 2016
Revised 29 December 2016
Accepted 9 January 2017

KEYWORDS
Crystalline silica; pulmonary toxicity; gene expression profile; toxicity mechanisms

Introduction

Silica, mainly because of its natural occurrence and abundance in earth's crust, is a major agent for occupational exposure. The National Institute for Occupational Safety and Health (NIOSH) recommended exposure limit (REL) for crystalline silica is 50 µg/m^3 (NIOSH, 2002). However, workers employed in specific occupations, for example, sand blasting, tunneling, silica milling, mining, construction and hydraulic fracturing (fracking) are more likely to be exposed to significantly higher levels of crystalline silica (Esswein et al., 2013; Radnoff et al., 2014) and, therefore, are at an excessive risk for developing adverse health effects from such exposures. Among the adverse health effects potentially resulting from excessive occupational exposure to crystalline silica, silicosis assumes major importance. Silicosis, an irreversible but preventable and potentially life-threatening progressive fibrotic lung disease, accounts for the death of over 100 workers/year in the US (Mazurek et al., 2015) and thousands of new cases are being reported worldwide annually (Leung et al., 2012). Besides silicosis, exposure to crystalline silica is associated with lung cancer (IARC, 1997), cardiopulmonary toxicity (Guo et al., 2016), mycobacterial infection (Pasula et al., 2009), kidney diseases (Vupputuri et al., 2012) and autoimmune diseases (Steenland & Goldsmith, 1995). Prevention of adverse health effects, specifically silicosis, associated with occupational exposure to crystalline silica is a major concern of NIOSH, OSHA, World Health Organization (WHO) and International Labor Organization (ILO). Since the current permissible exposure limits (PEL) for respirable crystalline silica do not adequately protect workers from developing adverse health effects associated with their occupational exposure to silica, the Occupational Safety and Health Administration (OSHA) has proposed to lower the PEL of respirable crystalline silica to 50 µg/m^3 of air as an eight-hour time-weighted average in all industries (OSHA, 2016). Significant progress has been made in silicosis prevention in the US primarily by controlling occupational exposure to dust containing respirable crystalline silica. Nevertheless, silicosis continues to be a problem in the US and worldwide. For example, in recent years, the incidence of silicosis in the US has increased with increased incidences of coal workers' pneumoconiosis

CONTACT Pius Joseph pcj5@cdc.gov Toxicology and Molecular Biology Branch, National Institute for Occupational Safety and Health (NIOSH), MS 3014, 1095 Willowdale Road, Morgantown, WV 26505, USA

Supplemental data for this article can be accessed here.

(Halldin et al., 2015). Additionally, patients are younger and develop accelerated, severe silicosis with higher mortality (Laney & Weissman, 2014).

Since silicosis is an irreversible and potentially fatal occupational disease, early detection of the disease at an asymptomatic stage has merit in its prevention (NIOSH, 2002). Additionally, a clear understanding of the mechanisms underlying the pulmonary effect(s) associated with silica exposure may be helpful in the prevention of adverse health effects potentially resulting from silica exposure. Our laboratory has been conducting studies, by employing a rat model for crystalline silica-induced pulmonary toxicity/silicosis, in an effort to develop minimally invasive biomarkers for early detection of silicosis as well as understanding the molecular mechanisms responsible for silica-induced pulmonary toxicity. Inhalation exposure of rats to crystalline silica (15 mg/m^3, six hours/day, five days) resulted in the induction of pulmonary toxicity which steadily progressed during the post silica-exposure time intervals up to 32 weeks (Sellamuthu et al., 2011a, 2012, 2013). The silica-induced pulmonary toxicity was accompanied by the induction of lung inflammation and a strong correlation was noticed between the progression of pulmonary toxicity and inflammation in our rat model (Sellamuthu et al., 2011a, 2013), further supporting the central role attributed to inflammation in the initiation and progression of silica-induced pulmonary toxicity (Castranova, 2004). Currently, by employing the same rat silica toxicity model, we have investigated the progression of pulmonary toxicity at a later post-silica exposure time interval of 44 weeks following termination of the five days of exposure to silica. Pulmonary toxicity was determined in the rats on the basis of BAL parameters of toxicity [LDH activity, number of alveolar macrophages (AMs) and polymorphonuclear (PMNs) neutrophils, and BAL level of the inflammatory cytokine, monocyte chemoattractant protein-1 (MCP-1)] and lung histology. Additionally, global gene expression profile was determined in the BAL cells and lung tissue of the control and silica exposed rats to determine the molecular mechanisms potentially underlying pulmonary toxicity detected in the silica exposed rats.

Materials and methods

Exposure of rats to crystalline silica aerosol

The entire animal study was conducted in an Association for Assessment and Accreditation of Laboratory Animal Care International approved animal facility (NIOSH, Morgantown, WV) in accordance with a protocol approved by the Institutional Animal Care and Use Committee. Approximately 3 months old, pathogen-free, male Fischer 344 rats (CDF strain) purchased from Charles River Laboratories (Wilmington, MA) were used in the study. The rats, following their arrival to the animal facility, were acclimated for about a week prior to their use in the study. The entire procedure for generation of an aerosol containing respirable crystalline silica and exposure of rats to the aerosol was conducted as described in our previous publications (Sellamuthu et al., 2011a, 2012). Stated briefly, a bulk supply of Min-U-Sil 5 silica (US Silica, Berkeley Springs, WV) was used in generating an aerosol using a modified version of a previously described system. An automated computer-controlled exposure system was used to deliver precise concentrations of uniformly dispersed airborne silica particles with a size distribution within the respirable range recommended for rats. The mass-median aerodynamic diameter of the airborne silica particles within the exposure chamber was 1.6 µm with a geometric standard deviation of 1.6 (Sellamuthu et al., 2011a). The target levels of temperature (22.2–25.6 °C), humidity (40–60%) and silica concentration (15 ± 1 mg/m^3) in the exposure chamber were monitored and controlled continuously by the exposure system. One group of rats ($n = 8$) was exposed to crystalline silica at a concentration of 15 mg/m^3, 6 h/day for five consecutive days. Another group of rats ($n = 8$) was exposed simultaneously to filtered air served as the controls. Compared to the REL of crystalline silica for workers, the concentration of silica present in the rat inhalation exposure chamber was 300-fold higher. Based on the estimated alveolar deposition, the total amount of silica deposited in the rat over the entire exposure period of five days corresponds to 2 years of deposition in a worker. Following exposure, the rats were maintained on a 12-hour light–dark schedule with free access to food and tap water for 44 weeks. The rats were monitored regularly for food and water intake and any symptom of toxicity. Weekly body weights of the rats were also recorded.

Euthanasia of rats and isolation of biospecimens

At 44 weeks following termination of the one week exposure to air or silica, the rats were euthanized with an intraperitoneal injection of ≥100 mg sodium pentobarbital/kg body weight (Fort Dodge Animal Health, Fort Dodge, IA). Blood drawn directly from the abdominal aorta was transferred to Vacutainer tubes (Becton-Dickinson, Franklin Lakes, NJ) containing EDTA as an anticoagulant and further processed to determine hematological parameters and global gene expression profiles as described below. The right lung of the rats was clamped off and bronchoalveolar lavage (BAL) was performed in the left lung as previously described (Sellamuthu et al., 2011a). The cellular and acellular fractions of the BAL fluid (BALF) collected from the left lung were used for further biochemical analysis of lung injury and inflammation and global gene expression profiling (see below for details). The diaphragmatic and cardiac lobes of the right lung were inflated and preserved in 10% neutral-buffered formalin for histopathological analysis of the lung injury while the apical lobe was chopped into small pieces and stored in RNAlater (Invitrogen, Carlsbad, CA) and used for gene expression studies as described below.

Biochemical analysis of pulmonary toxicity and inflammation

Lactate dehydrogenase (LDH) activity, a general indicator of pulmonary toxicity, and albumin content, an indicator of

alveolar epithelial integrity, were determined in the acellular fraction of BALF obtained from the rats using a COBRA MIRA autoanalyzer (Roche Diagnostic Systems, Mont Clair, NJ) as described previously (Porter et al., 2001). Protein concentration of the inflammatory cytokine, MCP-1 was determined in the acellular fraction of BALF using an ELISA kit (Invitrogen, Carlsbad, CA) and a Spectramax 250 plate spectrophotometer equipped with a Softmax Pro 2.6 software (Molecular Devices, Sunnyvale, CA). The cellular fraction of BALF was resuspended in 1 ml of phosphate buffered saline and the total number of AMs and PMN leukocytes was determined using a Coulter Multisizer II and Accu Comp software (Coulter Electronics, Hialeah, FL). 500 000 BAL cells were spun onto microscope slide using a Cytospin 3 centrifuge (Shandon Life Sciences International, Cheshire, UK) and stained with a Leukostat stain (Fisher Scientific, Pittsburgh, PA) to differentiate AM and PMN. Two hundred cells were counted per rat, and AM and PMN percentages were multiplied across the coulter counter total cell counts to obtain total AM and PMN numbers.

Hematology

The total and differential white blood cell (WBC) counts of the unclotted blood samples obtained from the control and silica exposed rats were determined by flow cytometer using blood cell-specific rat antibodies (BD Pharmingen, San Diego, CA). The leukocytes were separated into three gates (lymphocytes, monocytes and neutrophils) by forward and side scattering. After collecting 3500 counting beads, the data were analyzed using a FlowJo software (Treestar, Costa mesa, CA).

Lung histology

The diaphragmatic and cardiac lobes of the lungs preserved in 10% neutral buffered formalin were subsequently embedded in paraffin, sectioned at a thickness of 5 µm and stained with hematoxylin and eosin (H&E) or Masson's trichrome stain. The slides were assessed for histological changes (H&E stain) or fibrosis (Masson's trichrome stain) by a board-certified pathologist (Experimental Pathology Laboratory, Inc., Sterling, VA). The severity of lung fibrosis in the control and silica exposed rats was scored as none (0), minimal (+), mild (++), moderate (+++) or severe (++++).

RNA isolation

Total RNA was isolated from the apical lobe of the lungs and BAL cells which were preserved in RNAlater. The RNeasy Fibrous Mini Kit (Qiagen Inc., Valencia, CA) was employed to isolate total RNA from the apical lung lobe as described previously (Sellamuthu et al., 2012). Total RNA from the BAL cells was isolated using the RNeasy Mini Kit (Qiagen Inc., Valencia, CA) following the instructions provided with the kit. The RNA samples were digested with RNase-free DNase and further purified using the RNeasy Kit (Qiagen Inc., Valencia, CA). The integrity and purity of the RNA samples isolated from lungs and BAL cells were determined using the Agilent 2100 Bioanalyzer (Agilent Technologies, Palo Alto, CA) and RNA was quantitated by UV–vis spectrophotometry. Only RNA samples exhibiting an RNA Integrity Number (RIN) ≥ 8.0 were used in the determination of global gene expression profile.

Global gene expression profile

The global gene expression profiles in the RNA samples purified from the lungs and BAL cells of the control and silica exposed rats were determined using RatRef-12 V1.0 Expression BeadChip microarrays (Illumina, Inc., San Diego, CA). All microarray experiments were performed to comply with Minimal Information About a Microarray Experiment (MIAME) protocols. Biotin-labeled cRNA was generated from 375 ng RNA samples each by employing the Illumina TotalPrep RNA Amplification Kit (Ambion, Inc., Austin, TX). Chip hybridizations, washing, Cy3-streptavidin staining, and scanning of the chips on the BeadStation 500 platform (Illumina, Inc., San Diego, CA) were performed following the protocols provided by Illumina, Inc., San Diego, CA.

Metrics files from the bead scanner were checked to ensure that all samples fluoresced at comparable levels before samples were loaded into Beadstudio (Framework version 3.0.19.0) Gene Expression module v.3.0.14. Housekeeping, hybridization control, stringency and negative control genes were checked for proper chip detection. BeadArray expression data were then exported with mean fluorescent intensity across like beads and bead variance estimates into flat files for subsequent analysis.

Illumina BeadArray expression data were analyzed in Bioconductor using the "lumi" and "limma" packages. Bioconductor is a project for the analysis and comprehension of genomic data and operates in R, a statistical computing environment (Ihaka & Gentleman, 1996). The "lumi" Bioconductor package was specifically developed to process Illumina microarrays and covers data input, quality control, variance stabilization, normalization and gene annotation (Gentleman et al., 2004). Normalized data were then analyzed using the "limma" package in R. In short, limma fits a linear model for each gene, generates group means of expression, and calculates p values and log fold-changes which are converted to standard fold changes. The raw p values were corrected for false discovery rate (FDR) using the Benjamini and Hochberg procedure (Benjamini & Hochberg, 1995). Several test filters (fold changes in expression, FDR p values or combinations of both) were employed to select significantly differentially expressed genes (SDEGs) in the silica exposed rats compared to the controls.

Bioinformatic analysis of gene expression data

The SDEGs identified by applying the selection filter (fold change in expression >1.5 and FDR p value <0.01) were used as input for subsequent bioinformatics analysis using

Ingenuity Pathway Analysis (IPA, Ingenuity Systems, www.ingenuity.com). IPA software is designed to map the biological relationship of the uploaded genes and classify them into categories according to published literature in the database. Fisher's exact test was conducted to calculate p values to determine the significance of a particular biological function or canonical pathway enriched by silica exposure in the lungs and BAL cells ($p < 0.05$ was considered statistically significant).

Statistical analysis of the data

Non-microarray data between the silica exposed and the control group of rats were compared using the one-way ANOVA test. Post hoc comparisons were made with Fisher's least significant difference (LSD) test. The level of statistical significance was set at $p < 0.05$.

Results

Pulmonary toxicity in the silica exposed rats

No significant change was observed in the physical activity, food and water consumption, or body weight gain in the silica exposed rats compared to the control rats during the entire 44-week post-exposure period (data not presented). The BALF levels of both LDH and albumin in the silica exposed rats were approximately two-fold higher compared to the air exposed control rats (Figure 1(A,B)). These results suggest the induction of pulmonary toxicity in the silica exposed rats compared with the control rats. Results of histological analysis of the lungs further support the pulmonary toxicity induced by inhalation exposure of rats to crystalline silica (Figure 2). Two morphologically distinct areas, affected by their inhalation exposure to crystalline silica, were noticeable in the lungs of the rats. There was a minimal to moderate granulomatous inflammation consisting of a central area of large, tightly packed macrophages surrounded by variable numbers of lymphocytes. The granulomas were randomly distributed in the lung but in some cases were found expanding the pleura or bronchio-alveolar lymphoid tissue (BALT). The other affected area consisted of alveolar septa expanded by minimal to mild amounts of fibrosis (when examined with H&E) and lined by minimal to mild amounts of type-II pneumocyte hyperplasia. Intermixed was a minimal to mild amount of chronic-active inflammation consisting of few AMs, lymphocytes and neutrophils. Silica particles were undetectable in the lung sections when observed under polarized light. Very few silicotic nodules were detected in the lung sections of the silica exposed rats and there was no clear histological evidence for alveolar lipoproteinosis or histocytosis in the silica exposed rat lungs (data not presented). In addition, although alveolar fibrosis was apparent using H&E it was more evident when examined with Masson's trichrome. All exposed animals had mild to moderate amounts of fibrosis using the Masson's trichrome stain (Figure 2). The lung fibrosis was more severe (five rats had a score of "++" and three rats had a score of "+++") in these rats compared to an earlier, 32-week post-silica exposure time period (all the rats had a score of "+") (Sellamuthu et al., 2012).

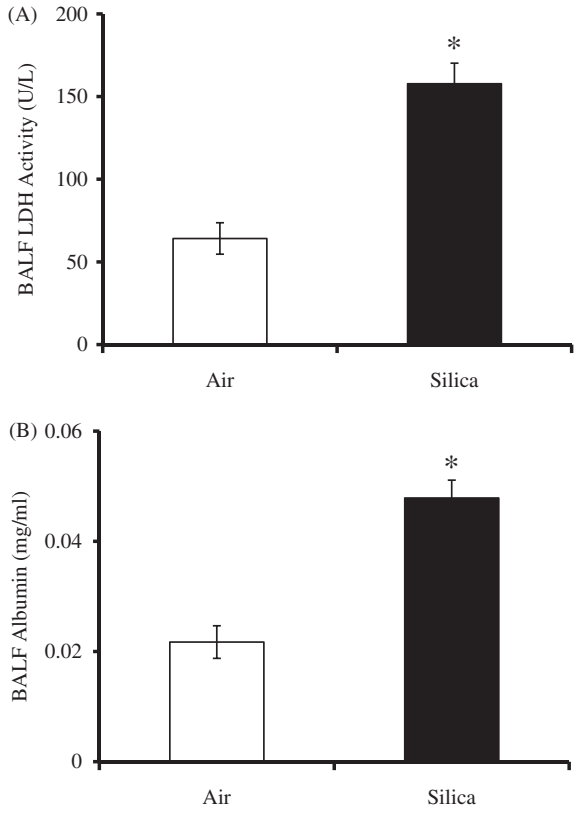

Figure 1. BALF parameters of pulmonary toxicity in rat lungs. Groups of rats were exposed by inhalation to filtered air or crystalline silica and LDH activity (A) and albumin content (B) were determined in the BALF as described in the text. Values represent mean ± S.E. ($n = 8$). *Statistically significant ($p < 0.05$) compared to the control rats.

Induction of inflammation in the silica exposed rats

Inhalation exposure of rats to crystalline silica, compared to air, resulted in a significant increase in the number of AMs (Figure 3(A)) and PMNs (Figure 3(B)) in their lungs suggesting the induction of pulmonary inflammation. A significant increase in the BALF concentration of the inflammatory chemokine, MCP-1, detected in the silica exposed rats, compared to the air controls (Figure 3(C)), further supports silica-induced pulmonary inflammation in rats. Silica exposure, in addition to pulmonary inflammation, resulted in systemic inflammation as evidenced by a significant increase in the number of neutrophils in the blood of the silica exposed rats compared to the controls (Figure 3(D)).

Global gene expression profile in lungs and BAL cells in the silica exposed rats

Microarray analysis of global gene expression profiles in the RNA samples isolated from the lungs and BAL cells detected 11 283 and 9177 transcripts, respectively, in the rats. Several selection filters were applied to the microarray data to identify genes in the lungs and BAL cells of the rats whose expression levels were significantly different in response to

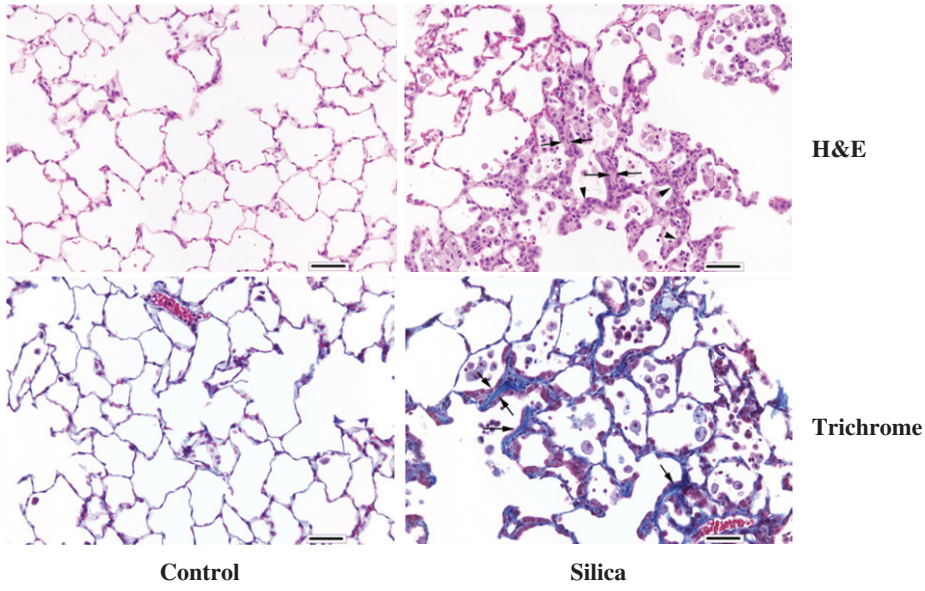

Figure 2. Photomicrographs of rat lungs. Lung samples from the control and silica exposed rats were sectioned and stained with H&E (top panel) or Mason's trichrome stain (bottom panel) as described in the text. In the H&E stained lung section of the silica exposed rat, the arrows show abundant type II pneumocyte hyperplasia and the smaller arrows show areas of alveolar fibrosis characterized by pink, fibrous material that lines the septa thickened by fibrosis compared to the control. The arrowhead in the trichrome stained sections shows 2–3 times thickened alveolar septa in the silica exposed rat lungs compared with the control. Magnification: ×200.

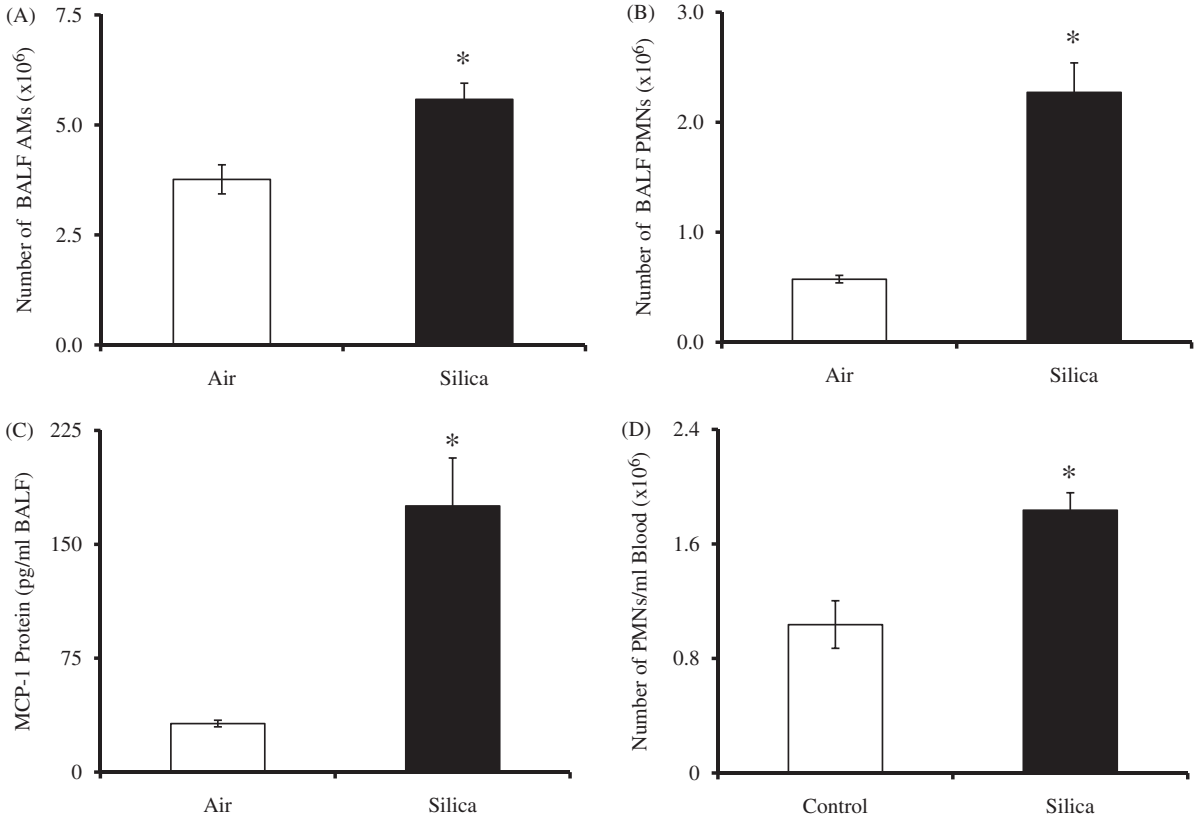

Figure 3. BALF and blood parameters of inflammation in rats. Groups of rats were exposed by inhalation to filtered air or crystalline silica and the total number of alveolar macrophages (A), infiltrating polymorphonuclear leukocytes (B) and concentration of MCP-1 (C) were determined in the BALF as described in the text. The number of neutrophils (D) in unclotted blood samples was also determined as described in the text. Values represent mean ± S.E. ($n = 8$). *Statistically significant ($p < 0.05$) compared to the control rats.

their exposure to crystalline silica. These included fold change in expression of >1.2, 1.5 and 1.8 and FDR p values of <0.05, 0.01 and 0.001. The number of SDEGs detected in the lungs and BAL cells when each of the selection criteria was applied is presented in Table 1. In general, the number of SDEGs (total, overexpressed and down-regulated) detected in the BAL cells outnumbered those detected in the lungs regardless of the selection filter employed.

Table 1. Number of significantly differentially expressed genes (SDEGs) in lung and BAL cells of silica exposed rats.

Selection criteria	Lungs			BAL cells		
	Total	Up	Down	Total	Up	Down
Fold change >1.2	874	462	412	1039	536	503
Fold change >1.5	124	114	10	232	151	81
Fold change >1.8	56	55	1	113	82	31
FDR $p < 0.05$	2209	1038	1171	3390	1564	1826
FDR $p < 0.01$	1116	558	558	2232	1083	1149
FDR $p < 0.001$	331	185	146	1232	631	601
Fold change >1.5 and FDR $p < 0.01$	94	87	7	225	150	75

Table 2. Fold changes in expressions and FDR p values of top 15 ranking SDEGs in lung tissues of silica exposed rats (a complete list of SDEGs is provided in Supplementary Table 1).

Gene name	Fold change in expression	FDR p value
Resistin like alpha	17.72	0.000005
Secreted phosphoprotein 1	9.45	0.00005
Solute carrier family 26, member 4	8.33	0.000014
Chitinase (presumed)	7.47	0.000012
Matrix metallopeptidase 12	4.56	0.000028
Ubiquitin D	4.47	0.0042
Chemokine (C–C motif) ligand 2	3.19	0.0000063
Complement factor I	3.17	0.000042
Similar to IG light chain Vk region Y13-259	2.65	0.0016
Complement component 4 binding protein, alpha	2.59	0.000040
Similar to immunoglobulin kappa-chain	2.58	0.0021
Immunoglobulin joining chain	2.55	0.00017
Similar to NGF-binding Ig light chain	2.52	0.00017
Fatty acid binding protein 4, adipocyte	2.41	0.00037
Similar to immunoglobulin kappa-chain VK-1	2.33	0.0042
Chemokine (C-X-C motif) ligand 9	2.31	0.0053
Similar to immunoglobulin kappa-chain	2.31	0.0059

Additionally, in general, the number of overexpressed genes was more than the number of down-regulated genes. Using a rather stringent selection filter consisting of a combination of fold change in expression >1.5 and an FDR p value <0.01, we identified 94 and 225 genes in the lungs and BAL cells, respectively, as significantly differentially expressed (Supplementary Tables 1 and 2). Fifteen of the SDEGs were found to be common between the lungs and BAL cells (Supplementary Table 3). The 15 top ranking SDEGs detected in the lungs and BAL cells of the silica exposed rats are presented in Tables 2 and 3, respectively.

Bioinformatic analysis of SDEGs detected in the lungs and BAL cells of silica exposed rats

Bioinformatic analysis of the SDEGs by IPA, in the lungs and BAL cells of the rats, provided insights into the mechanisms underlying the progression of pulmonary toxicity as detected by the biochemical (Figures 1 and 3) and histological (Figure 2) analysis of the control and silica exposed rats. Significant enrichment of a large number of IPA categories, in particular, diseases and biological functions and canonical pathways, was detected in the lungs and BAL cells of the rats in response to their inhalation exposure to crystalline silica. Findings of bioinformatic analysis of the gene expression data suggested the predominant involvement of inflammation in silica-induced pulmonary toxicity in rats and supported the findings of histological and biochemical

Table 3. Fold changes in expressions and FDR p values of top 15 ranking SDEGs in BAL cells of silica exposed rats (a complete list of SDEGs is provided in Supplementary Table 2).

Gene name	Fold change in expression	FDR p value
Apolipoprotein E	19.36	0.00000031
Secreted phosphoprotein 1	10.14	0.00005
Histocompatibility 2, class II antigen E alpha	7.83	0.00000028
Chemokine (C–C motif) ligand 7	7.48	0.00000051
RT1 class II, locus Db1	6.88	0.0000098
HOP homeobox	6.5	0.0000000026
Chemokine (C–C motif) ligand 2	6.12	0.0000013
Interleukin 1 receptor, type II	5.70	1.27E − 08
Schlafen 3	4.82	0.000000070
Lymphocyte antigen 6 complex, locus E	3.97	0.000000035
Secretory leukocyte peptidase inhibitor	3.90	0.000000056
Cd74 molecule, major histocompatibility complex, class II invariant chain	3.78	0.0000060
Matrix metallopeptidase 12	3.76	0.00015
Fibronectin 1	3.56	0.0000017
Leukocyte immunoglobulin-like receptor, subfamily B, member 4; similar to GP49B1	3.53	0.00000051

analysis of lung, BAL cells and BALF presented in Figures 1–3. The majority of the IPA diseases and biological function categories that were enriched in the lungs and BAL cells were related to inflammation (Figure 4 and Supplementary Tables 4 and 5). Cellular movement and cell-to-cell signaling and interaction were the top ranked IPA disease and biological function category in the lung and BAL cells, respectively. A remarkable similarity was observed in the IPA diseases and biological function categories significantly enriched in the lungs and BAL cells in spite of the differences in the individual SDEGs in the lungs and BAL cells. For example, the IPA disease and biological function categories ranked among the top 15 in both lungs and BAL cells of the silica exposed rats were the same (Supplementary Tables 4 and 5). On the other hand, granulocyte adhesion and diapedesis and agranulocyte adhesion and diapedesis were the only common canonical pathway categories that were common and ranked among the top 15 in the lungs and BAL cells (Figure 5 and Supplementary Tables 6 and 7). Nevertheless, a vast majority of the top ranked and significantly enriched canonical pathways in both the lungs and BAL cells were related to inflammation.

Discussion

Pulmonary exposure of murine models such as rats and mice to crystalline silica results in silicosis (Porter et al., 2004; Rabolli et al., 2011). Both in humans and murine models, neither continuous nor current exposure to crystalline silica is required for silicosis to develop. Epidemiological studies have demonstrated that silicosis may develop in humans long after cessation of their exposure to crystalline silica (Miller et al., 1998). Similarly, previous studies conducted in our laboratory (Sellamuthu et al., 2011a, 2012) and elsewhere (Porter et al., 2001, 2004) have demonstrated that pulmonary toxicity due to exposure to crystalline silica in rats progressed after cessation of silica exposure. In agreement with these reports, the current study findings showed that silica-induced pulmonary toxicity

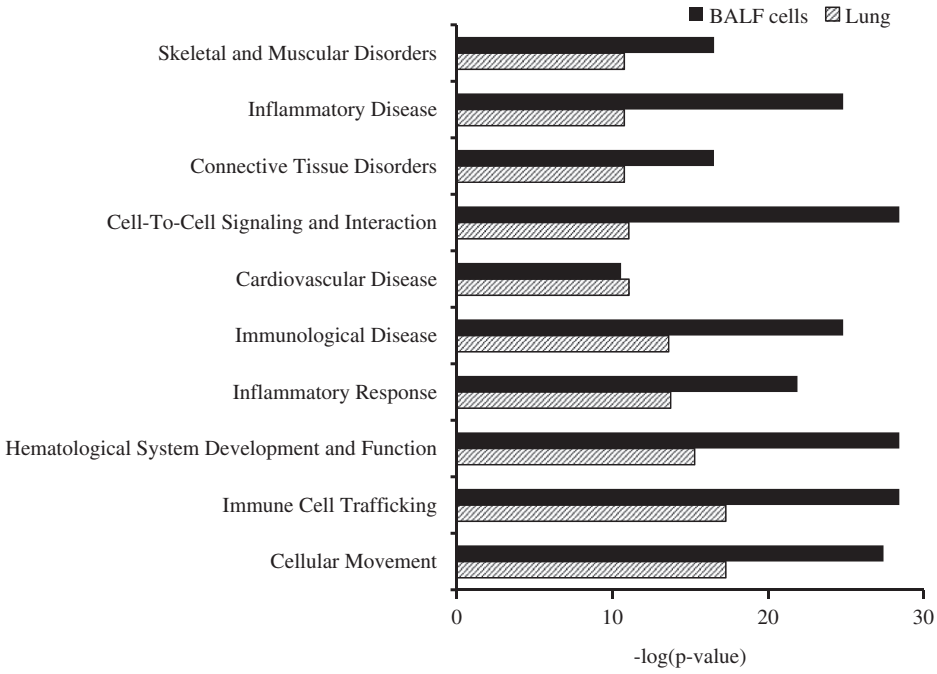

Figure 4. Biological function categories significantly enriched in the silica exposed rats. The SDEGs detected in the lungs and BAL cells ($n = 8$) were analyzed using the IPA software. The top 10 most significantly enriched diseases and biological functions in the lungs and corresponding categories in the BAL cells are presented. A complete list of the IPA diseases and biological function categories significantly enriched in the lungs and BAL cells of the silica exposed rats, compared to the controls, is presented in Supplementary Tables 4 and 5.

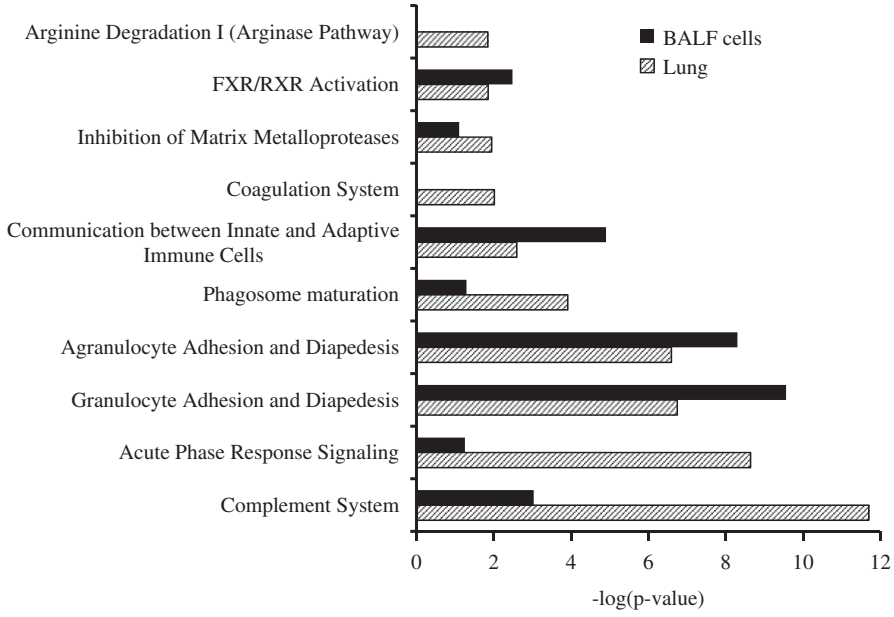

Figure 5. Canonical pathways significantly enriched in the silica exposed rats. The SDEGs detected in the lungs and BAL cells ($n = 8$) were analyzed using the IPA software. The top 10 most significantly enriched canonical pathways in the lungs and corresponding categories in the BAL cells are presented. A complete list of the IPA canonical pathways significantly enriched in the lungs and BAL cells of the silica exposed rats, compared to the controls, is presented in Supplementary Tables 6 and 7.

progressed during the post-exposure time interval of 44 weeks and culminated in lung fibrosis – a characteristic feature associated with silicosis.

Our laboratory has been conducting studies, by employing a rat model for silica-induced pulmonary toxicity, to determine the mechanisms underlying the initiation and progression of pulmonary toxicity following a one week inhalation exposure to crystalline silica. Previously, we have reported that inhalation exposure of rats to crystalline silica under exposure conditions identical to those employed in the current study resulted in mild pulmonary toxicity soon after termination of the one week exposure and a steady progress in the toxicity during the post-exposure time intervals up to 32 weeks (Sellamuthu et al., 2011a,b, 2012, 2013). Corresponding to the silica-induced pulmonary toxicity progression, a steady increase in the number of SDEGs in the lungs (Sellamuthu et al., 2013) and blood (Sellamuthu et al., 2011a) of the silica exposed rats,

compared with the time-matched controls, was detected. BALF LDH activity and albumen content, indicators of cytotoxicity and alveolar epithelial integrity, respectively, were significantly higher in the lungs of the silica exposed rats, compared with the controls (Figure 1(A,B)). These results, as expected based on the results of our previous studies (Sellamuthu et al., 2011a, 2012), suggested a moderate progression of pulmonary toxicity in the silica exposed rats at 44 weeks following the one week exposure to crystalline silica. Histological analysis of the lung samples obtained from the control and silica exposed rats, furthermore, supported the findings of biochemical analysis of BALF parameters of pulmonary toxicity. Type II pneumocyte hyperplasia, thickening of the alveolar septa, and positive staining to trichrome stain (Figure 2) indicated fibrotic changes, characteristic of silicosis (Porter et al., 2001), in the lungs of the rats in response to respirable crystalline silica exposure. The silica-induced pulmonary toxicity, in particular lung fibrosis, was more severe at the 44-week post exposure time period (Figure 2) compared to what we had previously reported for the 32-week post-exposure time period (Sellamuthu et al., 2012). Changes in lung parameters of inflammation such as MCP-1 level and the number of inflammatory cells in the BAL were lower at the 44 week post-silica exposure time interval compared to those reported for the 32 week post-exposure time interval (Sellamuthu et al., 2012). Many of the top ranking SDEGs detected at the 44 week time period in the rat lungs (Table 1) were also found significantly differentially expressed at earlier post-exposure time periods (Sellamuthu et al., 2012); however, the fold changes in expression, in general, were higher at the 44 week time period compared to those at the 32 week period.

Results obtained in this study clearly support the notion that chronic inflammation plays a central role in silica-induced pulmonary toxicity and silicosis (Castranova, 2004). A significant increase in the number of AMs, as detected in the lungs of the silica exposed rats (Figure 3A), is considered to be an adaptive response to engulf and thereby remove inhaled silica particles from the lungs to prevent toxicity (Misson et al., 2004). The significantly increased number of neutrophils infiltrating the lungs (Figure 3B), elevated BALF pro-inflammatory cytokine, MCP-1 (Figure 3C), and an increase in the number of WBCs in the blood (Figure 3D) suggest the induction of pulmonary and systemic inflammation in the silica exposed rats. In addition, lung histological changes detected in the silica exposed rats, compared with the controls (Figure 2), were consistent with a chronic-active inflammatory response as previously reported (Porter et al., 2004; Sellamuthu et al., 2012).

Progress made in toxicogenomics during the past few decades has demonstrated the importance of investigating gene expression changes taking place in target organs in response to exposure to toxic agents to study the toxicity of chemicals and particles (Hamadeh et al., 2002; Sellamuthu et al., 2011a, 2012). Gene expression profiling is useful to predict target organ toxicity since gene expression changes, in general, precede toxicity that can be detected by employing traditional biochemical and/or histological toxicity parameters (Heinloth et al., 2004; Sellamuthu et al., 2011a; Umbright et al., 2010). Additionally, bioinformatic analysis of the gene expression data provides valuable information regarding the mechanisms underlying target organ toxicity (Sellamuthu et al., 2012). The fate of crystalline silica particles entering the lungs, following inhalation exposure, depends on their interaction with the BAL cells and the lung tissue, especially the lung epithelium. Therefore, analysis of toxicity parameters in the BAL cells as well as the lungs is required to determine the full spectrum of silica-induced pulmonary toxicity in the rats. Similarly, global gene expression profiling of the BAL cells and lung tissue may provide insights regarding the mechanisms underlying silica-induced pulmonary toxicity as well as the contribution by the BAL cells and the lung epithelium individually and in combination to the overall pulmonary toxicity induced by inhaled silica. As expected, based on the results of previous studies (Sellamuthu et al., 2011b, 2012), inhalation exposure of rats to crystalline silica resulted in significant changes in the global gene expression profile of their lungs and BAL cells (Tables 1–3 and Supplementary Tables 1–3) in association with pulmonary toxicity (Figures 1–3) compared with the controls. The number of SDEGs detected in the BAL cells was more compared to the lungs (225 versus 94). This could be due to the fact that majority of the inhaled silica particles may not reach the lung epithelium since they are first engulfed by AMs present in the BAL for their detoxification. It is also possible that the interaction between silica particles and BAL cells is different from that between the particles and lung tissue possibly accounting for the differences in the gene expression profile observed in the BAL cells and lung tissue. Nevertheless, results of the bioinformatic analysis demonstrated considerable similarity in the biological functions (Figure 4) and canonical pathways (Figure 5) that were significantly enriched in response to silica exposure in the lung tissue and BAL cells.

It has been previously established that crystalline silica particles, upon their entry into the lungs, interact with AMs and alveolar epithelium to result in the induction of oxidative stress through generation of reactive oxygen species (ROS) (Porter et al., 2002), induction of inflammation (Porter et al., 2004), and induction of fibrosis (Porter et al., 2001) leading to silicosis. Several genes involved in the generation of ROS as well as the cellular response to the resulting oxidative stress, viz: superoxide dismutase 2 (*SOD2*), hemeoxygenase 1 (HMOX1), metallothionein 1A (*MT1A*), neutrophil cytosolic factor 1 (*NCF1*), NADPH oxidase organizer 1 (*NOXO1*), secreted phosphoprotein 1 (*SPP1*) and apolipoprotein E (*APOE*) were found significantly overexpressed in the lungs and/or BAL cells of the silica exposed rats compared with the controls (Supplementary Tables 1 and 2). In addition, bioinformatic analysis of the gene expression data identified a significant enrichment of the IPA disease and biological function category, free radical scavenging, in the lungs and BAL cells in response to silica exposure (Supplementary Tables 1 and 3). These findings are consistent with the involvement of oxidative stress as a mechanism in silica-induced pulmonary toxicity in our rat model (Castranova, 2004). It is quite likely that the

expression changes in the oxidative stress-related genes noticed in the rats at 44-weeks following termination of silica exposure are due to secondary effects of silica resulting in mitochondrial dysfunction (Hu et al., 2006).

Silicosis is often characterized as a chronic inflammatory and fibrotic pulmonary disease (Leung et al., 2012). The significant increase in the number of AM (Figure 3(A)) and PMN (Figure 3(B)) as well as elevated MCP-1 (Figure 3(C)) in the BAL and thickening of alveolar epithelium and trichrome staining (Figure 2) clearly indicated the induction of inflammation and fibrosis, respectively, in the silica exposed rats. The gene expression data obtained from the lung and BAL cell samples contributed mechanistic information toward the silica-induced pulmonary inflammation and fibrosis seen in the rats. Many of the IPA diseases and biological function categories and canonical pathways that were significantly enriched in the lungs and BAL cells of the silica exposed rats, compared with the controls, were inflammation related (Figures 4 and 5 and Supplementary Tables 1–4). Apolipoprotein E; Resistin like alpha (*RETNLA 1*); *SPP1*; solute carrier (SLC) family 26, member 4 (*SLC26A4*); and matrix metallopeptidase 12 (*MMP12*) were some of the top ranking SDEGs detected in the lungs and/or BAL cells of the silica exposed rats (Tables 2 and 3). Each of these genes is known to play significant roles in the pulmonary inflammation and fibrosis in response to exposure to toxic agents or under pathological conditions of known and unknown origin (see below for specific details). Therefore, it is reasonable to assume that the genes significantly affected by crystalline silica exposure in the current study, especially, *APOE, RETNLA1*, *SPP1*, *SlC26A4* and *MMP12*, are probably involved in maintenance and/or progression of pulmonary toxicity, in particular, inflammation (Figure 3) and fibrosis (Figure 2) in the rats. Many of these genes were also found significantly differentially expressed in the silica exposed rats at earlier post-exposure time intervals.

Among the SDEGs detected in the BAL cells of the silica exposed rats, the overexpression of *APOE* was most significant (Table 3). *APOE* maintains normal lipid homeostasis in lungs and other organs by facilitating the transport of cholesterol, triglycerides and phospholipids between blood and the cells (Yao et al., 2016). Additionally, *APOE* has been implicated to play a significant role in the pathogenesis of lung diseases. For example, a protective role for *APOE* against acute lung injury (Yamashita et al., 2014) and lung emphysema (Arunachalam et al., 2010) has been reported. The protective effect of *APOE* is primarily due to its ability to suppress inflammation, oxidative stress, and tissue remodeling and fibrosis as well as promote adaptive immunity and host defense (Naura et al., 2009). Crystalline silica, following inhalation exposure, is engulfed by AMs and, therefore, the very high overexpression of the protective gene, *APOE* detected in the BAL cells of the rats may be considered primarily a defense mechanism to prevent lung toxicity. However, the detection of significant pulmonary toxicity in the silica exposed rats, as supported by the results obtained from the BAL parameters of toxicity (Figures 1 and 3) and histology (Figure 2), may suggest that the *APOE*-mediated lung defense was overwhelmed in the silica exposed rats which facilitated in the induction of pulmonary toxicity.

RETNLA1, one of the members of a family of cysteine-rich secreted proteins, also referred to as resistin-like molecule (*RELM*), found in inflammatory zone 1 (*FIZZ1*) and hypoxia-induced mitogenic factor (*HIMF*) has been studied for its involvement in various lung diseases. *RETNLA1* is highly induced in a mouse chronic hypoxia model of pulmonary hypertension (Teng et al., 2003), and *RETNLA1* has multiple functions including mitogenic, angiogenic and vascular remodeling (Angelini et al., 2009; Teng et al., 2003; Yamaji-Kegan et al., 2006). *RETNLA1* is induced in lung allergic inflammation and bleomycin-induced pulmonary fibrosis (Liu et al., 2014). *RETNLA1* stimulates type 1 collagen and α-smooth muscle actin expression in lung fibroblasts is indicative of myofibroblast differentiation, a key feature in lung fibrosis (Xu et al., 2012). It is, therefore, reasonable to assume that the *RETNLA1* overexpression detected in the lungs of the silica exposed rats (Table 2) was, at least in part, responsible for the fibrosis detected in their lungs (Figure 2).

Osteopontin, a glycoprotein encoded by *SPP1* gene is often considered a biomarker for pulmonary inflammation and/or fibrosis (Pardo et al., 2005). *SPP1* was highly overexpressed in the BAL cells and lungs of the silica exposed rats (Tables 2 and 3). *SPP1* modulates immune function and extracellular matrix (ECM) remodeling (O'Regan, 2003), important features in the pulmonary response to crystalline silica exposure. A significant overexpression of *SPP1*, as noticed in the present study, has been reported under conditions of cigarette smoke-induced lung inflammation (Prasse et al., 2009) and asbestos-induced lung fibrosis (Sabo-Attwood et al., 2011). The molecular mechanisms underlying *SPP1*-mediated pulmonary inflammation and fibrosis involve alterations in pro-inflammatory chemokine/cytokine levels, immune cell profiles in BALF and lung, and mucin production in bronchioles (Sabo-Attwood et al., 2011). The association of osteopontin, the product of SPP1 gene, with granulomatous pathology together with the known properties of the protein, suggests the possible involvement of *SPP1* in granuloma formation such as that noticed currently in the silica exposed rats (Figure 2).

Several members of the SLC family of genes were found significantly differentially expressed in the BAL cells and lungs of the silica exposed rats compared with the air-exposed rats (Supplementary Tables 1 and 2). Among the significantly differentially expressed SLC family of genes, the overexpression of *SLC26A4* detected in the lung tissue was most profound and significant. The *SLC26A4* gene codes the protein, pendrin, which is responsible for excessive mucus production by airway epithelial cells (Nakao et al., 2008), and a definite relationship is known to exist between excessive mucus production by airway epithelial cells and morbidity and mortality from certain respiratory diseases (Rose & Voynow, 2006). Forced overexpression of pendrin results in the activation of the CXC family of cytokines and infiltration of neutrophils into lungs resulting in the induction of pulmonary inflammation (Nakao et al., 2008). We noticed a significant overexpression of several members of the CXC

family of chemokines (Supplementary Tables 1 and 2) and a significant increase in the number of infiltrating PMNs (Figure 3(B)) in the lungs of the silica exposed rats. These findings and those reported previously by Nakao et al. (2008) are consistent with the involvement of the *SLC26A4* gene in the progression of silica-induced pulmonary inflammation and toxicity in the rats. Currently, by employing a transgenic mouse model for the *SLC26A4* gene we are investigating the precise role, if any, of the *SLC26A4* gene in the initiation and progression of pulmonary toxicity in response to silica exposure.

Pulmonary fibrosis, characteristic of silicosis, is a complex process resulting from excess deposition of a collagen-rich ECM. The exact molecular mechanisms of pulmonary fibrosis, whether idiopathic in nature or under conditions of silicosis, are understood only to a limited extent. Matrix metalloproteinases (MMPs) are a family of proteins that play critical roles in cellular processes related to fibrosis such as cell migration, leukocyte activation and chemokine processing (Manicone & McGuire, 2008; Parks et al., 2004). MMPs are known to have both inhibitory and stimulatory roles in fibrosis (Giannandrea & Parks, 2014). *MMP12*, a prominent pro-fibrotic member of the MMP family of genes (Madala et al., 2010; Matute-Bello et al., 2007), was highly overexpressed in the lungs and BAL cells of the silica exposed rats compared with the controls (Tables 2 and 3). It has been demonstrated that *MMP12* influences fibroblast activation and collagen production (Kang et al., 2007) – processes critical in pulmonary fibrosis. The very high overexpression of *MMP12* in the BAL cells and lung samples obtained from the silica exposed rats (Tables 2 and 3) and the results of the histological analysis showing fibrosis in the same lung samples (Figure 2) suggest the involvement of *MMP12* in the fibrotic changes detected presently in the lungs of the silica exposed rats. However, whether *MMP12* mediated the fibrotic response in the silica exposed rats directly or through interaction with other genes in the lungs and/or BAL cells of the rats needs to be determined in future investigations.

In addition to the above described genes, several genes whose expression levels were significantly different in the lungs and BAL cells of the silica exposed rats also seem to have played important role(s) in the pulmonary toxicity detected in the rats. For example, the haptoglobin (*HP*) gene transcript was significantly overexpressed in the lungs of the silica exposed rats (Supplementary Table 1), and this may be considered as an adaptive response to protect the lungs against silica-induced pulmonary toxicity. Silica exposure results in hemolysis (Pavan et al., 2014) resulting in the release of heme and free hemoglobin (Hb) (Schaer et al., 2013). The free Hb, a pro-oxidant and pro-inflammatory molecule, in the absence of efficient detoxification, may accumulate in blood and tissue compartments to result in toxicity and tissue damage (Buehler et al., 2010). The binding of free Hb with HP to form Hb–HP complex is a major step involved in Hb detoxification which is mediated predominantly by hemeoxygenase (HMOX) (Schaer et al., 2014). The significant overexpression of both *HMOX* and *HP* transcripts seen in the lungs of the silica exposed rats (Supplementary Table 1) suggests an adaptive response to detoxify free Hb released by silica-mediated hemolysis. Many of the SDEGs noticed in the current study were also found significantly differentially expressed at early post-silica exposure time intervals in the silica exposed rats and the functional significance of their differential expression has been previously discussed (Sellamuthu et al., 2011a,b, 2012, 2013).

The toxicity and gene expression data presented in this study as well as in our previous publications (Sellamuthu et al., 2011a,b, 2012, 2013) demonstrating the involvement of inflammation as a major mechanism in silicosis are in agreement with the findings reported in several previous publications (Porter et al., 2004; Sellamuthu et al., 2012). A strong association has been reported between the degree of inflammatory cell recruitment and severity of lung fibrosis in response to silica exposure in rats (Porter et al., 2002, 2004; van Ravenzwaay et al., 2009). Up-regulation of several pro-inflammatory immune mediators including TNFα, IL-1β and IL-8 has been noticed in silica exposed rats in association with fibroblast activation and ECM production, further linking inflammation with pulmonary fibrosis (Barbarin et al., 2005). Administration of anti-inflammatory steroids blocked both silica-induced inflammation and fibrosis, therefore, supporting the critical role played by inflammation in silicosis (Barbarin et al., 2005; DiMatteo & Reasor, 1997). However, the involvement of inflammation in silicosis has been disputed in a number of studies conducted especially in mouse models of lung fibrosis. For example, Rabolli et al. (2011) have reported that lung fibrosis is not driven by inflammatory lung responses in NMRI mice. Similarly, IL-10 deficient mice exposed to silica developed only mild pulmonary fibrosis in spite of developing strong alveolitits (Huaux et al., 1998). The observation that fibrogenic but not pro-inflammatory genes are upregulated in a Lewis rat model of chronic silicosis prompted Langley et al. (2011) to question the role of inflammation in pulmonary fibrosis.

By employing the same rat model, we have previously reported that the silica-induced pulmonary toxicity correlated well with the induction of lung inflammation during the early post-silica exposure time intervals up to 32 weeks (Sellamuthu et al., 2011a,b, 2012, 2013). These findings were in agreement with the notion that inflammation plays a central role in silica-induced pulmonary toxicity including silicosis (Castranova, 2004). However, the findings reported in the present study suggest a potential disconnect between lung fibrosis and pulmonary inflammation at the late 44-week post-exposure time period. It is noteworthy that the increase in BALF MCP-1, a pro-inflammatory cytokine, in the silica exposed rats at 44-week post-exposure time interval was markedly lower (a 5.47-fold increase; Figure 3) compared to that was detected at the 32-week post-exposure time interval (a 16.33-fold increase; Sellamuthu et al., 2012). Similarly, the increase in the number of AMs and infiltrating PMNs in the lungs of the silica exposed rats, compared to the time-matched controls, at the 44-week post-silica exposure time interval (Figure 3(A,B)) was much lower compared to what was noticed at the 32-week post-silica exposure time interval (Sellamuthu et al., 2012). However, lung fibrosis in

the rats at 44 weeks (Figure 2) was more severe compared with the 32 weeks (Sellamuthu et al., 2012). The significance of this observation is not fully understood presently. The observation that the BALF MCP-1 level as well as the number of AMs and PMNs in the BAL increased steadily during the early post-silica exposure time period and peaked at 32 weeks, the time point at which lung fibrosis was first detected in our rat silicosis model, may suggest that inflammation was required, at least, for the initiation and early progression of pulmonary fibrosis. It is not known, however, whether continued inflammation is essential for maintaining and/or further progression of pulmonary fibrosis in the silica exposed rats. Investigations using advanced stages of lung fibrosis in rats beyond the 44-week post exposure time interval as well as pharmacological intervention of inflammation and/or the use of transgenic models for inflammation or fibrosis may help to determine precisely the involvement of inflammation, if any, in the initiation and progression of pulmonary fibrosis induced by inhalation exposure to crystalline silica.

Acknowledgements

The authors thank Amy Cumpston, Jared Cumpston and Howard Leonard (NIOSH, Morgantown, WV) for assistance with inhalation exposure of rats to crystalline silica.

Disclosure statement

The authors report no declaration of interest.

The findings and conclusions in this report are those of the authors and do not necessarily represent the views of NIOSH.

The microarray data have been deposited in the Gene Expression Omnibus Database, http://www.ncbi.nlm.nih.gov/geo (accession number GSE41572).

References

Angelini DJ, Su Q, Yamaji-Kegan K, et al. (2009). Hypoxia-induced mitogenic factor (HIMF/FIZZ1/RELMalpha) induces the vascular and hemodynamic changes of pulmonary hypertension. Am J Physiol Lung Cell Mol Physiol 296:L582–93.

Arunachalam G, Sundar IK, Hwang JW, et al. (2010). Emphysema is associated with increased inflammation in lungs of atherosclerosis-prone mice by cigarette smoke: implications in comorbidities of COPD. J Inflamm (Lond) 7:34.

Barbarin V, Nihoul A, Misson P, et al. (2005). The role of pro- and anti-inflammatory responses in silica-induced lung fibrosis. Respir Res 6:112.

Benjamini Y, Hochberg Y. (1995). Controlling the false discovery rate: a practical and powerful approach to multiple testing. J R Stat Soc Ser 57:289–300.

Buehler PW, D'Agnillo F, Schaer DJ. (2010). Hemoglobin-based oxygen carriers: from mechanisms of toxicity and clearance to rational drug design. Trends Mol Med 16:447–57.

Castranova V. (2004). Signaling pathways controlling the production of inflammatory mediators in response to crystalline silica exposure: role of reactive oxygen/nitrogen species. Free Radic Biol Med 37:916–25.

DiMatteo M, Reasor MJ. (1997). Modulation of silica-induced pulmonary toxicity by dexamethasone-containing liposomes. Toxicol Appl Pharmacol 142:411–21.

Esswein EJ, Breitenstein M, Snawder J, et al. (2013). Occupational exposures to respirable crystalline silica during hydraulic fracturing. J Occup Environ Hyg 10:347–56.

Gentleman RC, Carey VJ, Bates DM, et al. (2004). Bioconductor: open software development for computational biology and bioinformatics. Genome Biol 5:R80.

Giannandrea M, Parks WC. (2014). Diverse functions of matrix metalloproteinases during fibrosis. Dis Model Mech 7:193–203.

Guo J, Shi T, Cui X, et al. (2016). Effects of silica exposure on the cardiac and renal inflammatory and fibrotic response and the antagonistic role of interleukin-1 beta in C57BL/6 mice. Arch Toxicol 90:247–58.

Halldin CN, Reed WR, Joy GJ, et al. (2015). Debilitating lung disease among surface coal miners with no underground mining tenure. J Occup Environ Med 57:62–7.

Hamadeh HK, Bushel PR, Jayadev S, et al. (2002). Prediction of compound signature using high density gene expression profiling. Toxicol Sci 67:232–40.

Heinloth AN, Irwin RD, Boorman GA, et al. (2004). Gene expression profiling of rat livers reveals indicators of potential adverse effects. Toxicol Sci 80:193–202.

Hu S, Zhao H, Al-Humadi NH, et al. (2006). Silica-induced apoptosis in alveolar macrophages: evidence of in vivo thiol depletion and the activation of mitochondrial pathway. J Toxicol Environ Health A 69:1261–84.

Huaux F, Louahed J, Hudspith B, et al. (1998). Role of interleukin-10 in the lung response to silica in mice. Am J Respir Cell Mol Biol 18:51–9.

Ihaka R, Gentleman R. (1996). R: a language for data analysis and graphics. J Comput Graph Stat 5:299–314.

International Agency for Research on Cancer (IARC). (1997). IARC monographs on the evaluation of carcinogenic risk to humans: silica, some silicates, coal dust and para-aramid fibrils. Vol. 68. Lyon, France: World Health Organization, International Agency for Research on Cancer.

Kang HR, Cho SJ, Lee CG, et al. (2007). Transforming growth factor (TGF)-beta1 stimulates pulmonary fibrosis and inflammation via a Bax-dependent, bid-activated pathway that involves matrix metalloproteinase-12. J Biol Chem 282:7723–32.

Laney AS, Weissman DN. (2014). Respiratory diseases caused by coal mine dust. J Occup Environ Med 56:S18–S22.

Langley RJ, Mishra NC, Pena-Philippides JC, et al. (2011). Fibrogenic and redox-related but not proinflammatory genes are upregulated in Lewis rat model of chronic silicosis. J Toxicol Environ Health A 74:1261–79.

Leung CC, Yu IT, Chen W. (2012). Silicosis. Lancet 379:2008–18.

Liu T, Yu H, Ullenbruch M, et al. (2014). The in vivo fibrotic role of FIZZ1 in pulmonary fibrosis. PLoS One 9:e88362.

Madala SK, Pesce JT, Ramalingam TR, et al. (2010). Matrix metalloproteinase 12-deficiency augments extracellular matrix degrading metalloproteinases and attenuates IL-13-dependent fibrosis. J Immunol 184:3955–63.

Manicone AM, McGuire JK. (2008). Matrix metalloproteinases as modulators of inflammation. Semin Cell Dev Biol 19:34–41.

Matute-Bello G, Wurfel MM, Lee JS, et al. (2007). Essential role of MMP-12 in Fas-induced lung fibrosis. Am J Respir Cell Mol Biol 37:210–21.

Mazurek JM, Schleiff PL, Wood JM, et al. (2015). Notes from the field: update: silicosis mortality – United States, 1999–2013. MMWR Morb Mortal Wkly Rep 64:653–4.

Miller BG, Hagen S, Love RG, et al. (1998). Risks of silicosis in coal workers exposed to unusual concentrations of respirable quartz. Occup Environ Med 55:52–8.

Misson P, van den Brule S, Barbarin V, et al. (2004). Markers of macrophage differentiation in experimental silicosis. J Leukoc Biol 76:926–32.

Nakao I, Kanaji S, Ohta S, et al. (2008). Identification of pendrin as a common mediator for mucus production in bronchial asthma and chronic obstructive pulmonary disease. J Immunol 180:6262–9.

Naura AS, Hans CP, Zerfaoui M, et al. (2009). High-fat diet induces lung remodeling in ApoE-deficient mice: an association with an increase in circulatory and lung inflammatory factors. Lab Invest 89:1243–51.

NIOSH. (2002). Hazard review: health effects of occupational exposures to respirable crystalline silica. US Department of Health and Human Services (NIOSH) Publication No. 2002-129. Available from: http://www.cdc.gov/niosh/docs/2002-129/02-129a.html.

Occupational Safety and Health Administration (OSHA). (2016). Occupational exposure to respirable crystalline silica; final rule. Available from: www.federal register.gov/articles/2016/03/25/2016-04800/2016-04800/occupational-exposure-to-respirable-crystalline-silica. [Last accessed: 6 Sep 2016].

O'Regan A. (2003). The role of osteopontin in lung disease. Cytokine Growth Factor Rev 14:479–88.

Pardo A, Gibson K, Cisneros J, et al. (2005). Up-regulation and profibrotic role of osteopontin in human idiopathic pulmonary fibrosis. PLoS Med 2:e251.

Parks WC, Wilson CL, Lopez-Boado YS. (2004). Matrix metalloproteinases as modulators of inflammation and innate immunity. Nat Rev Immunol 4:617–29.

Pasula R, Britigan BE, Turner J, Martin WJ. 2nd. (2009). Airway delivery of silica increases susceptibility to mycobacterial infection in mice: potential role of repopulating macrophages. J Immunol 182:7102–9.

Pavan C, Rabolli V, Tomatis M, et al. (2014). Why does the hemolytic activity of silica predict its pro-inflammatory activity? Part Fibre Toxicol 11:76.

Porter DW, Hubbs AF, Mercer R, et al. (2004). Progression of lung inflammation and damage in rats after cessation of silica inhalation. Toxicol Sci 79:370–80.

Porter DW, Millecchia L, Robinson VA, et al. (2002). Enhanced nitric oxide and reactive oxygen species production and damage after inhalation of silica. Am J Physiol Lung Cell Mol Physiol 283:L485–93.

Porter DW, Ramsey D, Hubbs AF, et al. (2001). Time course of pulmonary response of rats to inhalation of crystalline silica: histological results and biochemical indices of damage, lipidosis, and fibrosis. J Environ Pathol Toxicol Oncol 20:1–14.

Prasse A, Stahl M, Schulz G, et al. (2009). Essential role of osteopontin in smoking-related interstitial lung diseases. Am J Pathol 174:1683–91.

Rabolli V, Lo Re S, Uwambayinema F, et al. (2011). Lung fibrosis induced by crystalline silica particles is uncoupled from lung inflammation in NMRI mice. Toxicol Lett 203:127–34.

Radnoff D, Todor MS, Beach J. (2014). Occupational exposure to crystalline silica at Alberta work sites. J Occup Environ Hyg 11:557–70.

Rose MC, Voynow JA. (2006). Respiratory tract mucin genes and mucin glycoproteins in health and disease. Physiol Rev 86:245–78.

Sabo-Attwood T, Ramos-Nino ME, Eugenia-Ariza M, et al. (2011). Osteopontin modulates inflammation, mucin production, and gene expression signatures after inhalation of asbestos in a murine model of fibrosis. Am J Pathol 178:1975–85.

Schaer DJ, Buehler PW, Alayash AI, et al. (2013). Hemolysis and free hemoglobin revisited: exploring hemoglobin and hemin scavengers as a novel class of therapeutic proteins. Blood 121:1276–84.

Schaer DJ, Vinchi F, Ingoglia G, et al. (2014). Haptoglobin, hemopexin, and related defense pathways-basic science, clinical perspectives, and drug development. Front Physiol 5:415.

Sellamuthu R, Umbright C, Li S, et al. (2011b). Mechanisms of crystalline silica-induced pulmonary toxicity revealed by global gene expression profiling. Inhal Toxicol 23:927–37.

Sellamuthu R, Umbright C, Roberts JR, et al. (2011a). Blood gene expression profiling detects silica exposure and toxicity. Toxicol Sci 122:253–64.

Sellamuthu R, Umbright C, Roberts JR, et al. (2012). Transcriptomics analysis of lungs and peripheral blood of crystalline silica-exposed rats. Inhal Toxicol 24:570–9.

Sellamuthu R, Umbright C, Roberts JR, et al. (2013). Molecular insights into the progression of crystalline silica-induced pulmonary toxicity in rats. J Appl Toxicol 33:301–12.

Steenland K, Goldsmith DF. (1995). Silica exposure and autoimmune diseases. Am J Ind Med 28:603–8.

Teng X, Li D, Champion HC, Johns RA. (2003). FIZZ1/RELMalpha, a novel hypoxia-induced mitogenic factor in lung with vasoconstrictive and angiogenic properties. Circ Res 92:1065–7.

Umbright C, Sellamuthu R, Li S, et al. (2010). Blood gene expression markers to detect and distinguish target organ toxicity. Mol Cell Biochem 335:223–34.

van Ravenzwaay B, Landsiedel R, Fabian E, et al. (2009). Comparing fate and effects of three particles of different surface properties: nano-TiO(2), pigmentary TiO(2) and quartz. Toxicol Lett 186:152–9.

Vupputuri S, Parks CG, Nylander-French LA, et al. (2012). Occupational silica exposure and chronic kidney disease. Ren Fail 34:40–6.

Xu H, Yang F, Sun Y, et al. (2012). A new antifibrotic target of Ac-SDKP: inhibition of myofibroblast differentiation in rat lung with silicosis. PLoS One 7:e40301.

Yamaji-Kegan K, Su Q, Angelini DJ, et al. (2006). Hypoxia-induced mitogenic factor has proangiogenic and proinflammatory effects in the lung via VEGF and VEGF receptor-2. Am J Physiol Lung Cell Mol Physiol 291:L1159–68.

Yamashita CM, Fessler MB, Vasanthamohan L, et al. (2014). Apolipoprotein E-deficient mice are susceptible to the development of acute lung injury. Respiration 87:416–27.

Yao X, Gordon EM, Figueroa DM, et al. (2016). Emerging roles of apolipoprotein E and apolipoprotein A-I in the pathogenesis and treatment of lung disease. Am J Respir Cell Mol Biol 55:159–69.